



AN IMPROVED SPREAD PLASTICITY MODEL FOR INELASTIC ANALYSIS OF R/C. FRAMES SUBJECTED TO SEISMIC LOADING

Michael KYAKULA¹ and Sean WILKINSON²

SUMMARY

This paper proposes an improved spread plasticity model that correctly identifies the initiation of yielding anywhere in the beam, takes into account the gradual spread of plasticity, the shift of the points of contraflexure, the variable location and actual length of the yield zones. The model assumes that columns and beam column joints remain elastic. Beams are made up of elastic and spread plasticity sub elements connected in series. When a beam yields, its stiffness reduces and flexibility increases. Before yielding spread plasticity sub element has a null matrix, as the beam yields, the magnitude of its coefficients increase. At each time step, the model updates the flexibility matrices of the spread plasticity sub elements. Unlike existing spread and concentrated plasticity models, moments within the span are monitored and the effect of their yielding or “unyielding” taken into account.

A number of examples are presented that demonstrate the limitations of the existing spread plasticity models. The paper concludes that spread plasticity models that only consider plasticity at the beam column connections are only accurate for lower stories and structures where the applied/design gravity load < 0.8 . The examples also show that compared to existing spread plasticity models, the proposed model improves the accuracy in calculation of global displacements, joint rotations and inter story drift ratios by up to 25%, 69% and 55% depending on the ratios of applied/design gravity load and bottom/top reinforcement.

INTRODUCTION

A major problem in seismic analysis and design of reinforced concrete structures is the modelling of non-linear behaviour. All existing methods of seismic analysis and design suffer from limitations caused by modelling assumptions and therefore can benefit from improvements. One of the ways in which improvements can be effected is through experimental work and field observation of damaged or surviving structures during and after an earthquake. The other is to perform parametric studies of multi degree of freedom structures using more elaborate numerical models and analysis methods.

The most sophisticated modelling procedure is the finite element method. However the complexity of the behaviour and size of the problem limits its application to validation of simpler models applied to analysis of simple structures and beams rather than non-linear analysis of multi degree of freedom building structures. Riva [1]. On the other hand, the most accurate method of dynamic analysis is the time history analysis. This too is computationally expensive and its application is generally limited to models less sophisticated than finite element.

A frequently used approach for representing non-linear behaviour in time history analysis is the concentrated or lumped plasticity model. The concentrated plasticity model assumes that non-linearity is lumped in springs at member ends. However these models ignore the gradual spread of plasticity in the member and therefore over estimate the maximum beam rotation and lateral displacement of the structure. Filippou [2].

To improve on this approximation, spread plasticity models were developed. Soleimani [3], Roufaiel [4], Filippou [2] These assume that yielding starts at beam-ends and that yield zones of finite length spread inwards from there. However, the start of yielding and location of yield zones varies depending on the ratio of earthquake to the gravity load, the distribution of the reinforcement at the top and bottom of the member and along the length of the member. It is further influenced by the arching effect in the slab due to the contribution of the slab reinforcement to the moment at the top of the beam.

Thus the yield zones may be located:

- (a) At both ends of the beam.
- (b) In the span only
- (c) At one end only
- (d) In the span and at one of the ends.

Moreover there is a new thinking in capacity design to shift the yield zones away from the beam column interface, by providing more reinforcement at beam ends and through the joint. Abdel-Fattah [5]. This moves the plastic zones away from the beam-ends and minimises the breakdown of the joint core due to alternating bond stresses and diagonal cracks. Models that assume hinges form at ends of beams can not analyse structures designed in this way.

The spread plasticity model in its present form only caters for beams in the lower stories where the earthquake load is greater than gravity load, and therefore the yield zones form at beam-ends. For effective analysis and design of medium to high rise buildings in the seismic regions, there is need for a new model that caters for hinges (yield zones) that form in the span as well as at the beam-ends. Further more these hinges need to be able to spread as the member yields.

The Structural model

The structural model adopted is one proposed by Filippou [2], however since this work sought to improve only the spread plasticity model, it did not consider the effects of shear and interface bond slip. The model consists of column and beam elements.

Columns and the beam column joints are assumed adequately reinforced, confined and detailed so that they do not yield. The column element consists of the axial force and elastic bending sub elements. The stiffness matrices of these sub elements are transformed to global co-ordinates then added to obtain the column stiffness matrix.

The beam element consists of the elastic bending, elastic axial and the spread plasticity sub elements connected in series. The spread plastic sub element accounts for the gradual spread of plastic deformation in the member, the shift of the point of contra-flexure, the variable location and actual length of the yield zones. It consists of one or two inelastic regions of finite length where the plastic deformations take place. An infinitely rigid bar or bars connect the inelastic regions. Filippou [2]. The locations and length of the inelastic and the rigid bars varies depending on whether the combined moment due to gravity and earthquake load has exceeded the yield moment of the member.

When a member yields, its stiffness reduces (its flexibility increases). The flexibility matrix of the elastic sub elements does not change, while that of the spread plastic element is zero before yielding, and

increases with yielding. The flexibility of the beam is obtained by adding the flexibility matrices of the elastic bending and spread plastic sub elements. Thus the coefficients of beam flexibility matrix increase (or coefficients of beam stiffness matrix decreases) as yielding progresses along the beam. The flexibility matrix of the beam is inverted, transformed into global co-ordinates, then added to the global stiffness matrix of the axial sub element to obtain the global beam stiffness matrix.

The structural model is modified so that when analysed for horizontal loading, the deflections and moments include the P-delta effects. The modification consists of adding a fictitious column having negative lateral stiffness properties proportional to the storey gravity loading. Its effect is to reduce the horizontal stiffness of each storey so that the resulting increased deflection and increased member moments are a function of the gravity loading as well as lateral loading. Gaiotti [6],

The stiffness matrix K , of a free unsupported structure is obtained by assembling the P- delta effect K_g , column K_c , and beam elements K_b , stiffness matrices. The digitised ground acceleration record is adjusted by adding a zero at the beginning and increasing the duration by Δt so that for the first time step, the earthquake load is zero and only the gravity load is acting. Then the deformations, moments, shears and axial forces at joints are found as in normal static analysis using uncondensed stiffness matrix adjusted for support conditions. In subsequent time steps, the condensed stiffness matrix is used.

Stiffness of yield zones

The curvatures of beam sections may be calculated by two different methods. In one case, the curvature ϕ , is given by

$$\phi = (M/EI), \quad (1)$$

Where:

- M = Applied moment at the section
- E = Young's modulus for concrete
- I = Moment of inertia

In the other method, the curvature ϕ , was given by

$$\phi = (\epsilon_c / y_n) \quad (2)$$

Where:

- ϵ_c = Strain in outermost fibre of concrete in compression
- y_n = depth to the neutral axis from the outer most compressive fibre of concrete.

It has been shown that before cracking the two moment curvature curves derived from both methods coincide. After cracking but before yielding, there is very little difference between the curves. However after yielding the curvature given by $\phi = (\epsilon_c / y_n)$ increases greatly for a small increase in moment, this is because there is a large increase in strain after yielding yet the neutral axis depth does not decrease much. On the other hand, for the curvatures given by $\phi = (M/EI)$, the neutral axis depth and thus moment of inertia I , does not decrease much with the increasing moment therefore there is very little change in the slope of the curve after yield. Kyakula [7]

After yielding, both methods give widely different values. Taking the stiffness of the yield zone as the slope of the moment curvature section after yield given by $\phi = (\epsilon_c / y_n)$, gives a lower bound stiffness. And calculating the stiffness of the yield zone from $\phi = (M/EI)$ gives an upper bound stiffness. The true value lies between these two.

Existing spread plasticity models assume that the curvatures in the moment curvature relationships are calculated from $\phi = (\epsilon_c / y_n)$. A sketch of such a moment curvature diagram; OABC is shown in figure 1.

Before cracking the stiffness of the section is given by the slope of the line OD while the slope of the line AB gives the stiffness of the cracked section up to just after yielding. They further assume that the stiffness of the section at the end of the yield zone that has just reach yield is given by the slope of line OD which is the stiffness for an elastic beam. This is taken as equal to infinity. At the other end, the stiffness is assumed equal to that of the reloading curve, which is approximately equal to the slope of line AC. Then the stiffness of the yield zone is taken as the average of a section with infinite stiffness and that of the reloading curve. Filippou [2]

Assuming the section of the yield zone that has just reached yield has infinite stiffness results in overestimating the stiffness after yielding. A more accurate calculation would involve calculating the effective stiffness as the average of AB and AC. Therefore average stiffness K of the plastic zone is assumed to be the average stiffness of the section at yield and that at maximum moment M_o . Kyakula [7]. The stiffness K is given by:

$$\frac{1}{K} = \frac{1}{2} \left[\frac{1}{K_{ab}} + \frac{1}{K_o} \right] \quad (3)$$

Where:

$$K_{ab} = \frac{M_y - M_{cr}}{\phi_y - \phi_{cr}} \quad (4)$$

$$K_o = \frac{M_o - M_{cr}}{\phi_o - \phi_{cr}} \quad (5)$$

The slope S_y of BC; the moment curvature curve after yield is given by; $S_y = \tan \theta$

The assumption that the stiffness of the part of the beam that has not yielded is equal to the elastic stiffness of the beam is not true because most of it has cracked; Aktan [8]. Never the less this assumption has been used in this research because the aim was to address the spreading plasticity due to yielding of reinforcement. Accuracy could be improved further by adopting a spread-cracking model to address the often neglected cracked but not yielded part of the beam; Kyakula [7]

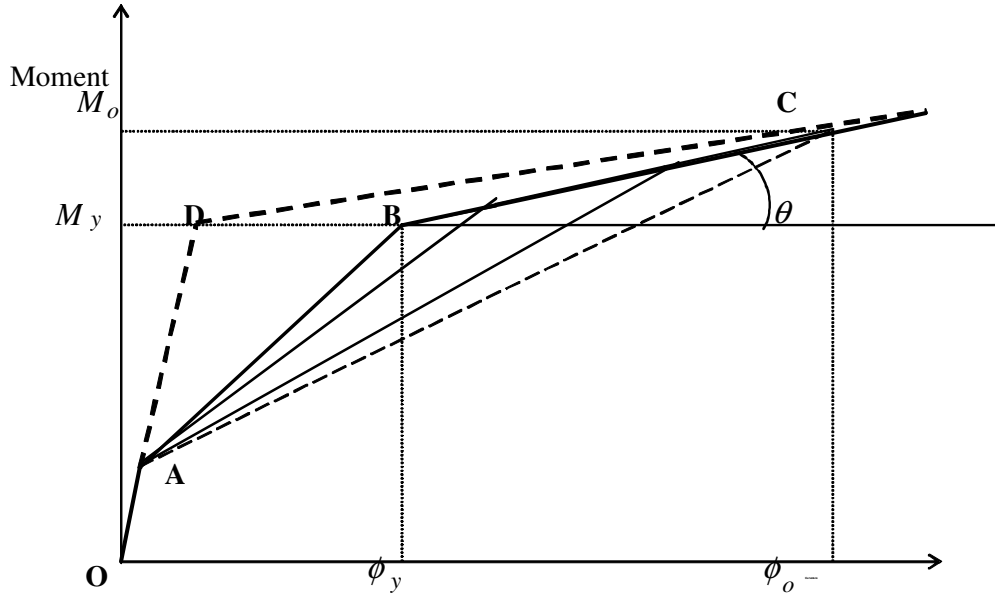


Figure 1 Stiffness of the Plastic Zone

Determination of the flexibility matrix of the spread plastic sub element

The derivation of the spread plasticity model involves determination of the formulae for the coefficients of the flexibility matrix of the spread plastic sub element of the beam. Yielding of any part of the beam or change in length of the yield zones changes the stiffness matrix of the structure. If the yield zone increases, the stiffness of the structure reduces (its flexibility increases). If the yield zone decreases, the stiffness of the member increases (its flexibility reduces). Before yielding the flexibility matrix of the spread plastic element is a null matrix. (Its elements are zero). As yielding increases, the magnitudes of the coefficients of its flexibility matrix increase. This section derives the formulae for coefficients of the flexibility matrix of the spread plasticity sub element for any length of yield zones formed anywhere in the beam by applying the principal of virtual work: External work WE is equal to internal work WI .

The flexibility matrix of the spread plastic sub-element for a beam with ends 1 and 2 may be written in the form;

$$[f]_{pl} = \begin{bmatrix} f_{11} & f_{21} \\ f_{12} & f_{22} \end{bmatrix} \quad (6)$$

The derivation of flexibility matrix follows the same procedure as given in Filippou [2] except that the general case of the sagging moment yield zone forming within the span near one of the beam ends, with the hogging moment yield zone forming at the beam column interface at the other end is considered. In the derivation, points A and B are the supports with more positive and less positive moment respectively, while C is the point of maximum sagging moment in the span – see Figure 2.

Coefficient f_{aa} is obtained by applying both the incremental moment and virtual unit moment at point A, while f_{bb} is found by applying the incremental moment and the virtual unit moment at end B.

Coefficient f_{ba} is found by applying an incremental moment at end B and the virtual unit moment at the point A. while f_{ab} is found by applying the moment increment at point A and the virtual unit moment at point B. If points A and 1 coincide, then $f_{11} = f_{aa}$, If the loading reverses such that points B and 1 coincide, then $f_{11} = f_{bb}$. And the other points follow accordingly.

An example for determination of one of the coefficients, such as f_{11} , where A and 1 coincide is illustrated in Figure 2.

The external work done is given by;

$$WE = f_{11}\Delta M_c \quad (7)$$

Internal work WI is given by:

$$WI = \int M(x)\Delta\phi(x)dx = \int M_u \frac{\Delta M_c}{K} dl = a_m \bar{M}_u \quad (8)$$

Where

$M(x)$ is the moment distribution due to the virtual unit moment at end A. It is given in Figure 2 (v).

$\Delta\phi(x)$ is the curvature distribution in Figure 2.(iv), due to the applied moment increment ΔM_A in Figure.2 (iii).

$$\Delta\phi(x) = \left(\frac{\Delta M_A}{K} \right) \quad (9)$$

Where:

K is the stiffness of the yield zone

M_u is the virtual unit bending moment diagram.

\bar{M}_u is the ordinate of the M_u diagram at the section through the centre of the curvature diagram.

a_m is the area of the curvature diagram.

K_c is the stiffness of the sagging moment yield zone in the span, K_b is the stiffness at hogging moment yielded zone at end B. It is assumed that the current lengths of the plastic zones in the span and at end, B are Z_c, Z_b respectively.

Where

$$Z_c = X_2 - X_1 \text{ and } Z_b = L - X_3.$$

L is the clear span of the beam.

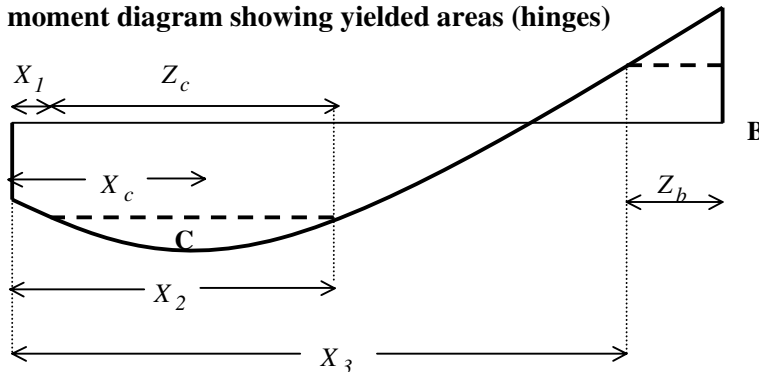
X_1 is the length from the beam column interface with the more positive bending moment to the first point where the sagging moment is equal to the yield moment.

X_c is the length from the beam column interface with the more positive bending moment to the point of the most positive moment in the beam.

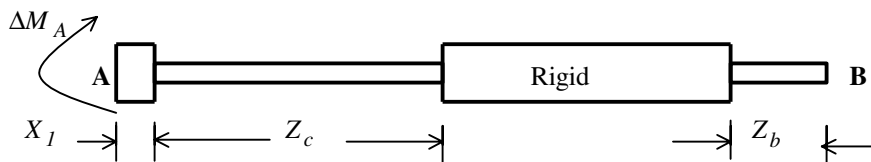
X_2 is the length from the beam column interface with the more positive moment to the second point where the moment is equal to the sagging yield moment

X_3 is the length from the beam column interface with the more positive moment, to the point where the moment is equal to the hogging yield moment.

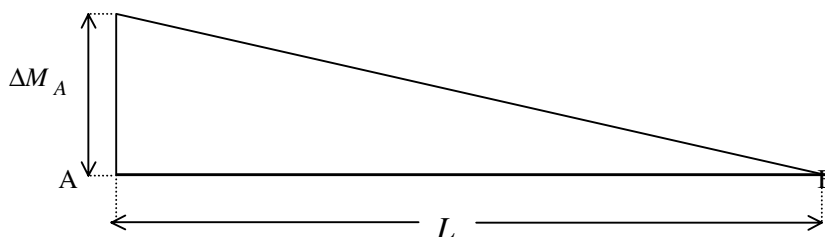
(i) Bending moment diagram showing yielded areas (hinges)



ii) Spread plastic sub-element



(iii) Real action, (bending moment diagram), due to moment applied at end A



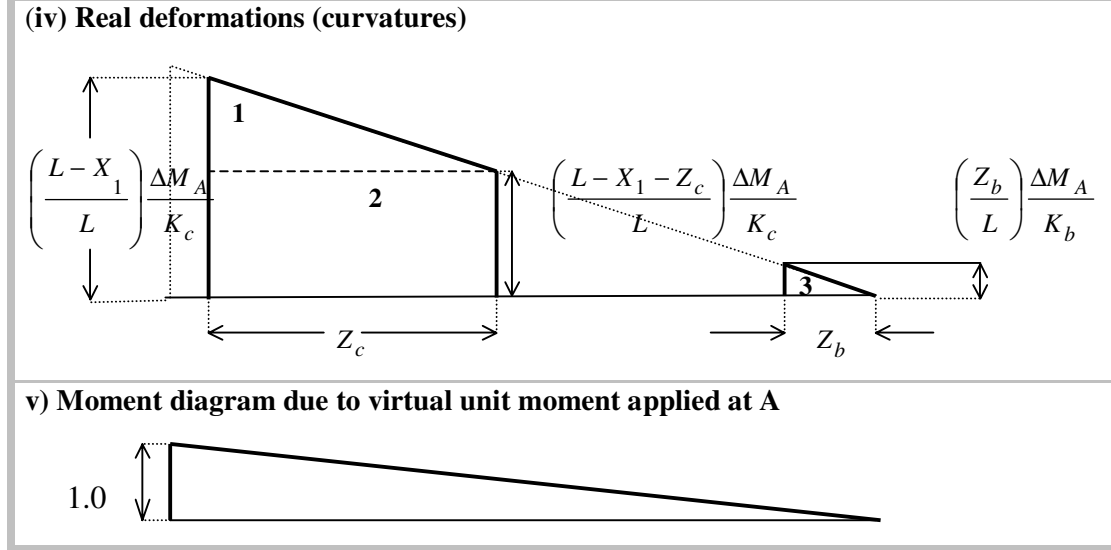


Figure 2: Derivation of f_{11} when hinges form in the span and at one end

The method for determination of yield zone length and location X_1, X_2, X_3, X_c is explained in references; Kyakula [7.9].

The curvature diagram in Figure 2(iv) is divided into three parts; therefore the internal work done is given by;

$$WI = \sum_{i=1}^3 a_{mi} \bar{M}_{ui} \quad (10)$$

$$\text{Let; } \mu = \frac{X_1}{L}, \quad \gamma_c = \frac{1}{K_c}, \quad \gamma_b = \frac{1}{K_b}, \quad \beta_b = \frac{Z_b}{L}, \quad \beta_c = \frac{Z_c}{L}$$

Substituting the above values in the equation for internal work and equating Internal work; WI and external work; $WE = f_{11} \Delta M_A$, gives;

$$f_{11} = \frac{L}{6} \left\{ 2\gamma_c \left[3\beta_c (1-\mu)^2 + (3\mu\beta_c^2 - 3\beta_c^2 + \beta_c^3) \right] + \left[2\gamma_b \beta_b^3 \right] \right\} \quad (11)$$

$$f_{22} = \frac{L}{6} \left\{ 2\gamma_b \left[3\beta_b - 3\beta_b^2 + \beta_b^3 \right] + 2\gamma_c \left[3\beta_c \mu^2 + 3\beta_c^2 \mu + \beta_c^3 \right] \right\}. \quad (12)$$

$$f_{21} = f_{12} - \frac{L}{6} \left\{ \gamma_c \left[6\mu\beta_c (1-\mu-\beta_c) + (3\beta_c^2 - 2\beta_c^3) \right] + \gamma_b \left(3\beta_b^2 - 2\beta_b^3 \right) \right\} \quad (13)$$

When the yield zones in the span reach the end of the beam; $\mu = X_1/L = 0.0$ Substituting this value in equations (11) to (13), the expressions for coefficients of the flexibility matrix $f_{11}, f_{22}, f_{21}, f_{12}$ reduce to those derived by Filippou [2], Soleimani [3]. The only difference arises from the value of the stiffness of the yielded zones used. These are reproduced below as equations (13), (14), (15).

$$f_{11} = \frac{L}{6} \left\{ 2\gamma_c \left[3\beta_c - 3\beta_c^2 + \beta_c^3 \right] + 2\gamma_b \beta_b^3 \right\} \quad (14)$$

$$f_{22} = \frac{L}{6} \{2\gamma_b [3\beta_b - 3\beta_b^2 + \beta_b^3] + 2\gamma_c \beta_c^3\} \quad (15)$$

$$f_{21} = f_{12} = \frac{-L}{6} \{ \gamma_c (3\beta_c^2 - 2\beta_c^3) + \gamma_b (3\beta_b^2 - 2\beta_b^3) \} \quad (16)$$

Similarly other cases of yield zone locations can be easily considered. For example

- (a) When yield zones form only in the span, $\beta_b = 0.0$.
- (b) When the yield zone is located only at beam end under the action of hogging moments, $\beta_c = 0.0$.
- (c) Where the yield zone is located only at beam end under the action of sagging moments, $\beta_b = 0.0$ and $X_l = 0.0$.

EXAMPLE

The aim of the example is to investigate the behaviour and performance of the structure based on the existing and proposed spread plasticity model. It seeks to show the variation of the location of the point of first yield in the span with the storey number and applied gravity load. It also shows the effect of varying the gravity load on the computed deformations given by different models. The stiffness of yield zone is determined in the same way for all models.

The structural frame

The sketch of the single bay five-storey frame used in analysis is shown in Figure 3. The frame is fixed at the base and, consists of columns that are 3.5m high and 0.4m square. The beams are 8 m long, 0.6m deep with a web width of 0.3m and effective flange width of 2.1m. It carries a floor slab that is 4.0m wide and 0.2m deep. The effective flange width b given by; $b = h + 3b_w$; Pantazopoulou [10] The frame was first designed according to Eurocode 8 using a gravity loads; $43kN/m$. The gravity load was obtained by considering the dead, imposed and partition loads.

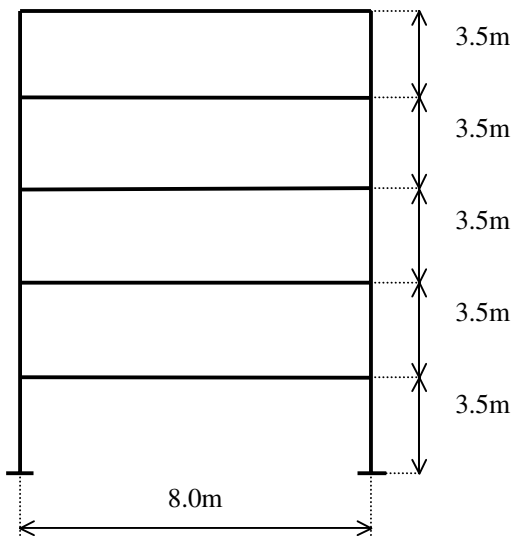


Figure 3: Five storey single bay frame sketch

The Ground Acceleration

The ground acceleration was provided by a simple half cycle sine wave in Figure 4. The ground acceleration A at any time is given by:

$$A = K \sin\left(\frac{2\pi}{T}t\right) \quad (16)$$

The value of K can be any reasonable number; in the Figure 3, $K = 1.0$. The dynamic load of $4 \sin(2\pi/T)$, was chosen after applying the various dynamic loads varying from $2 \sin(2\pi/T)$ to $6 \sin(2\pi/T)$, and it gave the inter storey drift ratio within the range recommended in literature: Moehle [11], Sattary-Javid [12]. The aim of using a simple dynamic loading was to facilitate study and easy comparison of the deformations of the structure resulting from application of both the existing and proposed spread plasticity models.

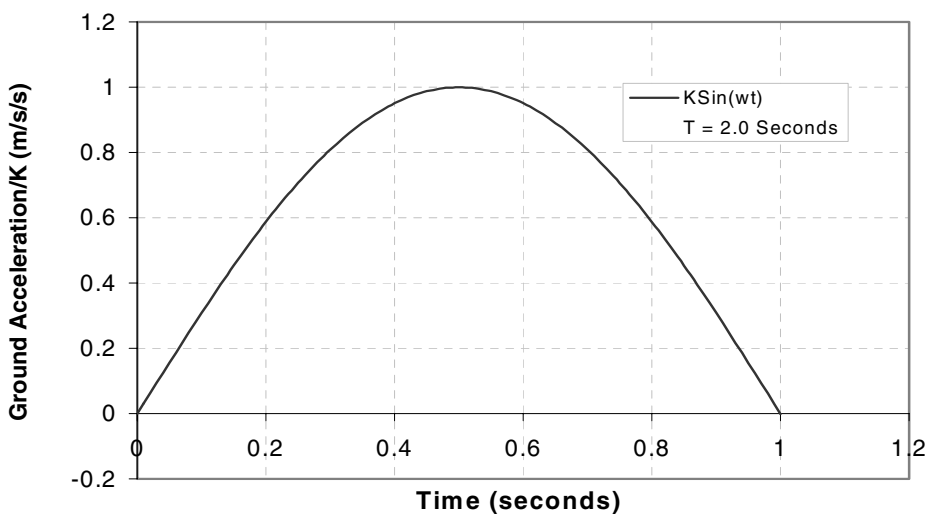


Figure 4: Simple Half Cycle Sine wave Ground Acceleration

Frame Design

A design of the frame must be made before any time history analysis can be carried out. And since it was assumed that the yielding of reinforcement identifies the onset of plasticity, the amount and distribution of reinforcement greatly influences the behaviour of the member. Therefore the discussion of the design of the frame is important in understanding their response. The designs for the frame was made according to Eurocode 8.[13] The floor beams carried a gravity load of 43kN/m made up of dead load and imposed loads. A pseudo spectral acceleration of approximately 0.5g was used in design. The columns and beam column joints were assumed not to yield.

The Eurocode 8 [13] divides the specification for structure into those designed and detailed to a high degree of ductility, DC “H”, medium ductility, DC “M”, and low ductility, DC “L”. In this example only DC “H” structures are considered. Two important aspect of beam design in Eurocode 8 affect the distribution of the reinforcement and thus the behaviour of the beam, and these are;

Clause 2.7.1.3.(b) of Eurocode 8 requires that “In critical regions, at least the50% of the amount of actual tension reinforcement is placed in the compression zone”. This clause aims at achieving ductility in the critical regions. Penelis[14]

Clause 2.7.2.3.(3)P requires that; “Within the critical regions, tension reinforcement ratio ρ shall not exceed the value ρ_{max} for DC “H” derived as follows;”

$$\rho_{max} = 0.35 \frac{f_{cd}}{f_{yd}} \frac{\rho'}{\rho} + 0.0015. \quad (17)$$

Where:

f_{cd} is the characteristic strength of concrete.

f_{yd} is the characteristic strength of reinforcement.

ρ' is the compression reinforcement ratio.

The two clauses imply that the minimum acceptable ratio of compression to tension reinforcement is 0.5. Also where this ratio exceeds ρ_{max} , and both the characteristic strength of reinforcement and concrete are not changed, the only design option is to keep the amount of tension reinforcement constant while that of the compression reinforcement is increased. In this case the characteristic strength of concrete and reinforcement were kept constant at $40N/mm^2$ and $460N/mm^2$ respectively.

Effect of gravity load on initiation of yield zone location

The variation of the point of initiation of yielding due to sagging moments with floor level and applied / design gravity load was investigated. The gravity load was varied as 0.7, 0.8, 0.9, 1.0, 1.1 and 1.2 times the design gravity load of $43kN/m$ while the dynamic load was kept constant at $4 \sin(2\pi/T)$. The time step used was 0.01 seconds. The fundamental period of the structure varied from 2.2s to 2.7s for the applied/ design gravity load ratio varying from 0.7 to 1.2. The length from the left-hand side support to the point where the sagging moment in the span first reached or exceeded the yield moment was plotted for the various gravity loads and for each floor level of the beam. These are given in Figure 5. From the figure it is seen that for values of applied/ design gravity load that are lower than 0.9 and for lower floor levels yielding started at the beam column interface. For higher ratios of applied to design gravity load, the yielding started in the span; in some cases about 2.0m from the support.

The existing spread plasticity models can not identify the start of yielding in the span and this causes them to underestimate the structural deformation. Also these models do not accurately compute the yield zone length and thus limit its maximum value to $0.25L$, where L is the clear span length. Soleimani [3], Filippou [2].

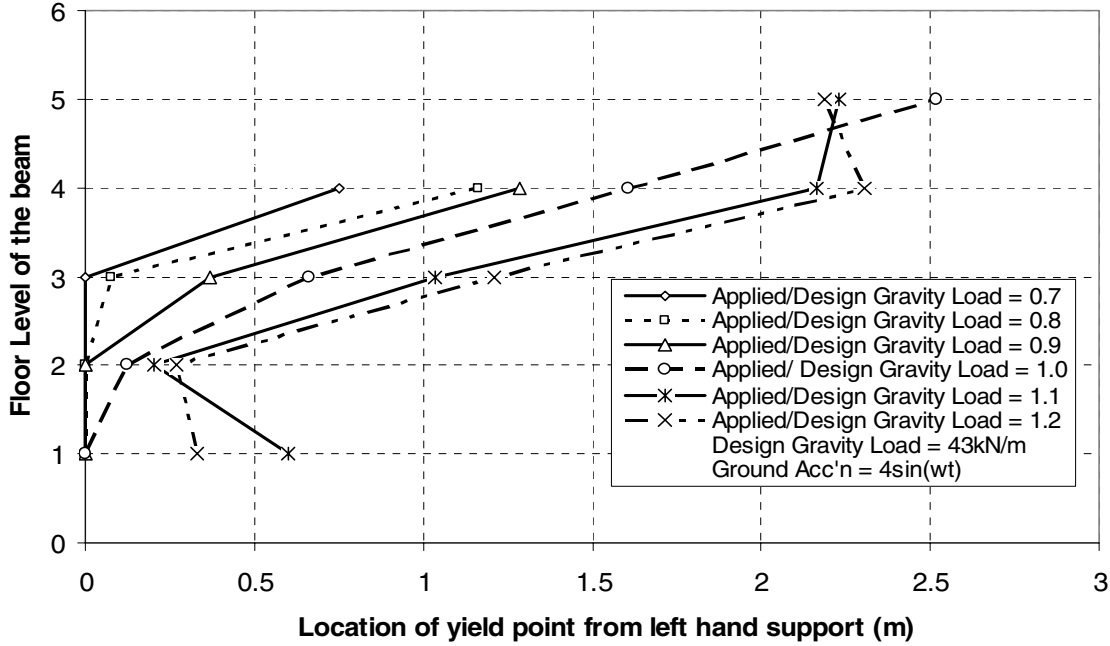


Figure 5: Location of yield point at the initiation of sagging moment yielding in the span

Effect of gravity load on maximum floor and roof Deflection

The effect of the gravity load on the maximum floor deflection was investigated. The full results for this investigation are given in Kyakula [7], only a few examples are reported here. The percentage improvement in determination of these deflections is given as:

$$IM \% = \left(\frac{\delta_p - \delta_e}{\delta_p} \right) \times 100 \quad (18)$$

Where

δ_p is deflections due to proposed model

δ_e is deflections due to existing model

$IM\%$ is a measure of the percentage improvement of the proposed model over the existing spread plasticity models.

Figure 6 shows the percentage improvement of the proposed model over the existing model due to Filippou [2], in calculation of the maximum floor deflection using for the frame with the design gravity load of $43kN/m$. It is seen that the percentage improvement increases with increasing applied/design gravity load ratio A_d , and increasing floor level. This is because for upper storeys, and higher ratios of applied/design gravity load, yielding starts in the span. Failure by the existing spread plasticity models causes errors. The errors in lower floors are due to failure by the existing models to calculate the length of yield zones accurately.

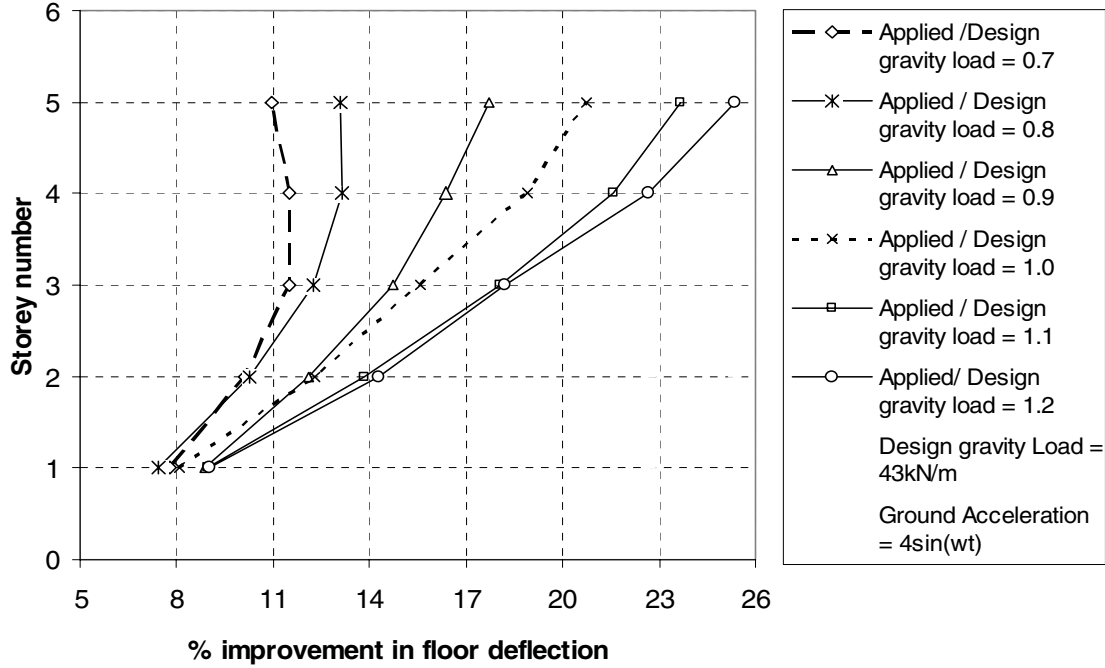


Figure 6: Percentage improvement in floor deflection

Joint Rotations

Figure 6 shows percentage improvement in calculation of maximum rotation for the right hand joints of the frame. It is seen to vary with the floor level and applied gravity load. Since at the application of dynamic load, the rotations are not equal to zero, but to a rotation θ_0 due to applied gravity load, the percentage improvement in determination of the rotations is given as:

$$IM \% = \left(\frac{\left(\theta_p - \theta_0 \right) - \left(\theta_e - \theta_0 \right)}{\left(\theta_p - \theta_0 \right)} \right) \times 100 \quad (19)$$

Where

θ_p is deflections due to proposed model

θ_e is deflections due to existing model

$IM\%$ is a measure of the percentage improvement of the proposed model over the existing spread plasticity models.

It is seen that the improvement in calculation of joint rotations increases with increasing ratio of applied/design gravity load. It also increases with increasing floor level, but tends to decrease for the top floors. This is because for upper storeys, and higher ratios of applied/design gravity load, yielding starts in the span. The reduction is because the moment in the span of upper storey beams has just reached yield or has not yielded at the onset of unloading.

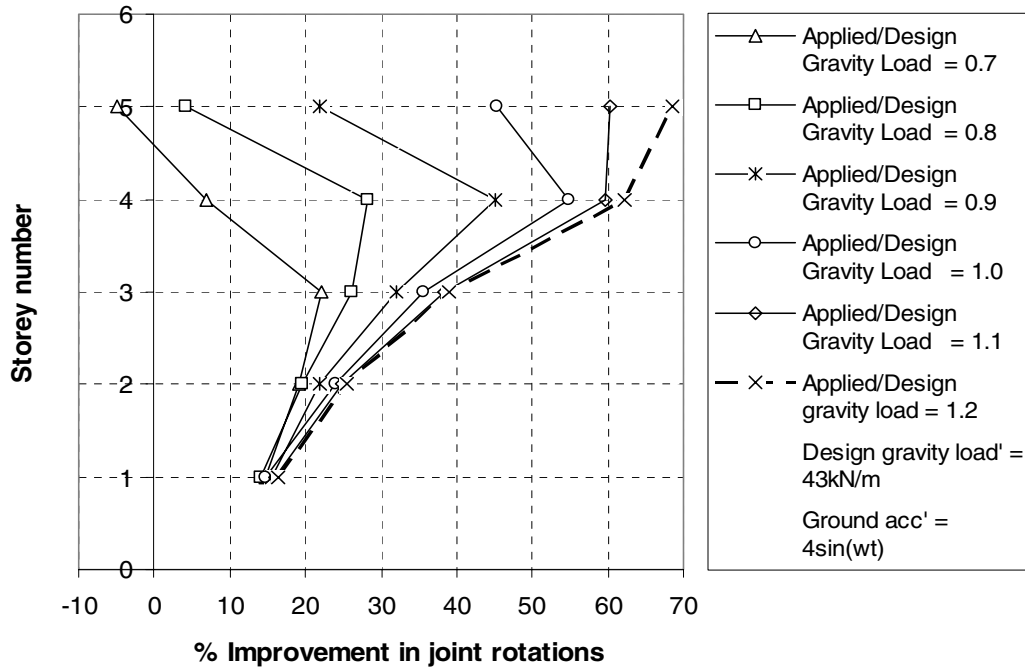


Figure 7; Percentage improvement in joint rotations

Maximum inter storey drift ratios

The maximum inter-storey drift ratios for all floors do not occur at the same time during the dynamic loading of the structure. Yet inter storey drift ratios should relate to the state of damage of the structure at a given time. Thus the maximum inter-storey drift ratios are defined as a set of inter storey drift ratios for all floors at a time when the highest value of inter-storey drift ratio occurs. Figure 7 shows the percentage improvement in maximum inter storey drift ratios as it varies with the floor level and applied gravity load for the frame with the design gravity load of $43kN / m$.

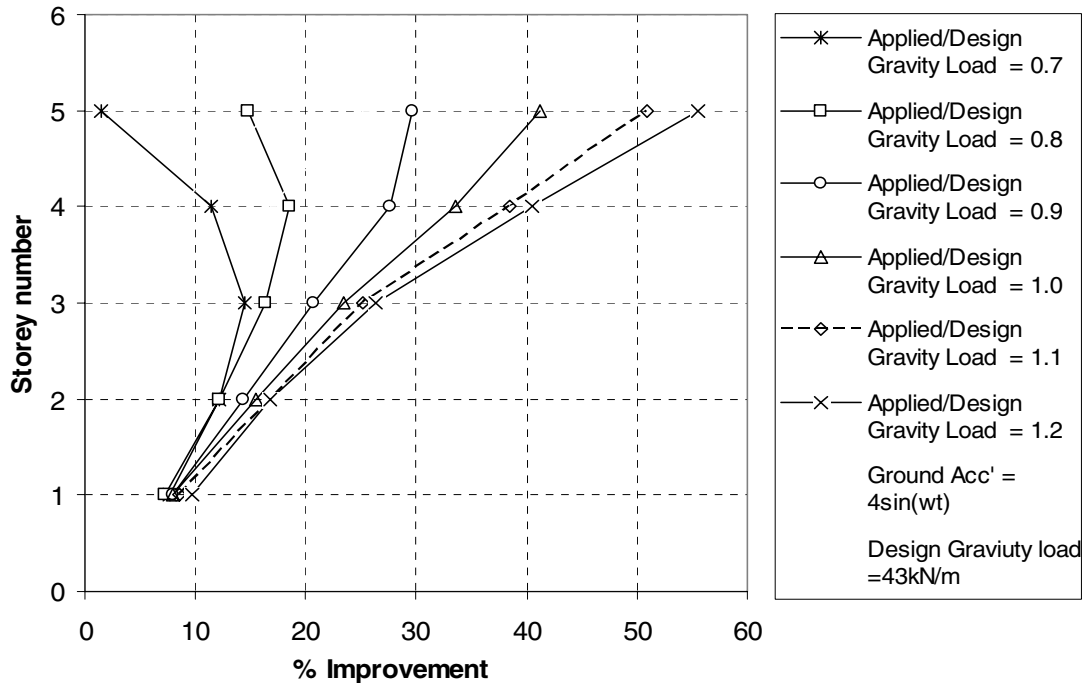


Figure 8: Percentage improvement in interstorey drift ratios

Generally cases where the yield zone has reached the end of the beam such as lower stories, the differences are small, caused by the failure of the existing models to accurately calculate the yield zone length. At upper floors, these differences are larger due to the failure of the existing models to recognise yield zones that form in the span. For lower applied/design gravity load, they reduce at roof level mainly because the sagging moment in the span has not reached yield

CONCLUSION

An improved spread plasticity model that correctly identifies the initiation of yielding anywhere in the beam, takes into account the gradual spread of plasticity, the shift of the point of contra-flexure, the variable location and actual length of the yield zones has been presented. The model accounts for the effects of gravity loads. A number of examples are presented that demonstrate limitations of the existing spread plasticity models. It is concluded that spread plasticity models that only consider plasticity at the beam column connections are only accurate for lower stories and structures where the gravity load is small compared to the seismic load. The examples also show that compared to existing spread plasticity models, the proposed model improves the accuracy in calculation of global displacements, joint rotations and inter story drift ratios by up to 25%, 69% and 55% depending on the ratios of applied/design gravity load.

REFERENCES

- 1) Riva, P and Cohn, M. Z. "Engineering approach to nonlinear analysis of concrete structures" Journal of Structural Engineering, 1990: 116(8): 2162-85.
- 2) Filippou, F. C. and Issa, A "Non linear analysis of reinforced concrete frames under cyclic load reversals." Report No NSF/ENG-88048, Earthquake Engineering research centre, University of California, Berkley, 1988.
- 3) Soleimani, D. Popov, E. P. and Bertero, V. V. "Nonlinear beam model for RC frame analysis", Seventh conference on electronic Computation, St Louis, Missouri, Aug 1979.

- 4) Roufaiel, M.S.L and Meyer, C. “Analytical modelling of hysteretic behaviour of RC frames” *Journal of Structural Engineering*, (1987); 113(3): 429-444.
- 5) Abdel-Fattah, B. and Wight, J. K. “Study of moving beam plastic hinging zones for earthquake resistant design of R/C buildings” *ACI structural journal*, 1987; 84-S4: 31-39
- 6) Gaiotti, R, Stafford Smith, B, “P-Delta analysis of building structures”, *Journal of Structural Engineering*, 1989; 115(4): 755-770.
- 7) Kyakula, M., “An improved Spread plasticity model for nonlinear Analysis of RC frames subjected to seismic loading” .PhD thesis, University of Newcastle upon Tyne, 2004
- 8) Aktan, A. E and Nelson G. E. “Problems in predicting seismic responses of RC buildings” *Journal of Structural Engineering*, (1988); 114(9): 2036-2055
- 9) Kyakula, M. & Wilkinson, S. M. “Effect of the length and location of yield zones on the accuracy of spread plasticity models”, 13th world conference on Earthquake Engineering, 2004; Vancouver, Canada
- 10) Pantazopoulou, S, J, Moehle, J. P and Shahrooz, B.M., “Simple analytical model for T-beams in flexure” *Journal of Structural Engineering*, 1988; 114(7): 1507-1523.
- 11) Moehle, J. P. and EERI, M. “displacement based design of RC structures subjected to Earthquakes” *Earthquake Spectra*, 1992; 8(3): 403-428
- 12) Sattary-javid, V and Wight J. K. “Earthquake load on R/C beams: Building versus single beam” *Journal of Structural Engineering*, 1986; 112(7): 1493-1507
- 13) EN, Eurocode 8, “Design and provisions for earthquake resistance of structures”. (1999)
- 14) Penelis, G. & Kappos,.; “Earthquake resistant concrete structures”, E & F N Spon, London, 1997

¹ Phd Student, University of Newcastle, Email: Michael.Kyakula@newcastle.ac.uk

² Lecturer University of Newcastle, Email: s.m.wilkinson@ncl.ac.uk